Available online at www.sciencedirect.com

ScienceDirect

Journal of Organometallic Chemistry 691 (2006) 4843–4849

Journal of Organometallic Chemistry

www.elsevier.com/locate/jorganchem

Electronic structures of permethyloligosilane radical cations at the ground and low-lying excited states

Hiroto Tachikawa [a,*], Hiroshi Kawabata [b]

[a] *Division of Materials Chemistry, Graduate School of Engineering, Hokkaido University, Sapporo 060-8628, Japan*
[b] *Department of Electronic Science and Engineering, Kyoto University, Kyoto 615-8510, Japan*

Received 12 June 2006; received in revised form 1 August 2006; accepted 2 August 2006
Available online 15 August 2006

Abstract

The electronic structures at the ground and low-lying excited states of permethyloligosilane radical cations, $Si_n(CH_3)_{2n+2}{}^+$ ($n = 4$–7), have been investigated using DFT and ab initio calculations. The calculations showed that positive charge (hole) is delocalized along the Si–Si main chain at the ground and first excited states. On the other hand, the hole is transferred to the methyl side-chain at the second and higher excited states. From these results, it was concluded that hole can move along the Si–Si main chain at thermal conditions. Also, it was predicted that intermolecular hole hopping takes place by photo-irradiation to the permethyloligosilane radical cation. The mechanism of hole transfer was discussed on the basis of the results.

Keywords: Radical cation; Oligosilane; Hole transport; Excited state; Ab initio CIS; DFT

---

1. Introduction

Polysilanes have been extensively investigated because of their potential utility as hole and electron transport materials in organic multilayer light emitting diodes (LEDs), one-dimensional semi-conductors, photo-resist materials, and high-density optical data storage materials [1–10]. These characteristic features are originated from high hole mobility of $10^{-4}\,cm^2\,V^{-1}\,s^{-1}$ and a low-lying excited state of polysilanes at doped state, which correlates strongly with the electron and hole conductivities as an organic semi-conductor. Hence, determination of the electronic structures of ionic states at both ground and excited states is an important theme in development of new materials of silane systems.

Charge transport in charge-injected polysilanes has been investigated extensively using time-of-flight [11,12] and time resolved microwave conductivity techniques [13–17]. The experiments indicate that thermal activation and field-assistance enhance hole mobility in polysilanes. The mobility of hole is as high as $10^{-4}\,cm^2\,V^{-1}\,s^{-1}$, while that of excess electron is a few order of magnitude lower. To elucidate mechanism of hole and excess electron transfers in polysilanes, several experiments have been carried out. Seki et al. measured [16] the transient absorption spectra of radical cations of a variety of substituted polysilanes by means of pulse radiolysis. It was suggested that phenyl rings bonded to the Si–Si skeleton are important in hole transport process between polymer chains. If the side chain is alkyl groups, hole mobility is significantly slower than in phenyl group. This is considered that spin densities on the phenyl group is larger than that of alkyl group. However, detailed mechanism for hole transport is still not clearly understood.

In the present, ab initio and density functional theory (DFT) calculations were applied to the oligosilane radical cation with methyl group in the side-chain to elucidate the mechanism of hole transport in oligosilane radical cation. In particular, we focus our attention on the hole transport processes at the low-lying excited states.

---

[*] Corresponding author. Fax: +81 11 706 7897.
E-mail address: hiroto@eng.hokudai.ac.jp (H. Tachikawa).

doi:10.1016/j.jorganchem.2006.08.008

It is known that spin density on the side-chain of radical ions of polysilane correlates strongly to charge transport and conductivity. If the spin density exists on the side chain, the hole hopping between polymer chains is possible via the side chain. On the other hand, if the spin density is localized only in the Si main chain, the hole transfer takes place along the intramolecular Si main chain. For example, the electron conductivity in radical anion of poly(methylphenylsilane) is significantly smaller than that of radical cation [18]. Electron spin resonance (ESR) and optical absorption spectra show that the spin density in the side-chain is close to zero in the radical anion, whereas that in the radical cation is larger than that of radical anion. The difference of charge conductivity is originated from the difference of spin densities in the side-chain. In the present study, we focus our attention on the difference of spin densities at the ground and excited states, and discuss the mechanism of hole conductivity in radical cation of permethyloligosilane.

2. Method of calculations

Almost all calculations were carried out at the DFT(B3LYP)/3-21G(d) level of theory. A linear oligosilane with methyl groups in side chain, permethyloligosilane ($Si_n(CH_3)_{2n+2}$) ($n = 4$–7), was examined as model of polysilane. For comparison, electronic states of phenylmethyloligosilanes were investigated.

First, the initial geometry of neutral oligosilane was made by MM2 calculation. Using the optimized geometry of the MM2 calculation, Next, direct molecular orbital–molecular dynamics (MO–MD) calculation was carried out for oligosilane to obtain the stable structure. The dynamics calculation was performed at semi-empirical PM3 level of theory. Using the geometries obtained by the MO–MD calculations, the structures of the oligosilane radical cations were fully optimized at the DFT(B3LYP)/3-21G(d) level of theory. Details of direct MO–MD calculations are described in recent our paper [19].

The excitation energies were calculated by means of time-dependent (TD)-DFT and singly excited configuration interaction (SE-CI) calculations. Six excited states were solved in these calculations. All hybrid DFT and ab initio calculations were carried out using GAUSSIAN03 program package [20]. Note that the similar levels of theory give reasonable features for several molecular device systems [21–23].

3. Results

3.1. Structures of oligosilanes ($n = 4$–7)

The geometrical structures of neutral and radical cation of oligosilane ($n = 4$–7) are fully optimized by means of the PM3 method. Using the optimized structures, direct MO–MD calculation is carried out to elucidate the effects of rotation of methyl group on the structure. Since previous experiments for the oligosilane radical cation have been performed mainly at 77 K, we chose 100 K for simulation temperature of oligosilane. As an example, snapshots of radical cation of oligosilane with $n = 7$ are illustrated in Fig. 1. At time zero, the oligosilane has a regular all-transoid structure. By thermal activation, methyl groups are freely rotated, but change of Si–Si skeleton is not large. After 4.0 ps, the structure of oligosilane is deformed, but the all-transoid structure is not changed. The distance between head and tail silicon atom of $n = 7$ is plotted as a function of time in Fig. 2A. At time zero, the distance is 11.34 Å. This distance vibrates in the range 11.10–11.85 Å during the simulation, indicating that the all-transoid structure is kept at 100 K. Temperature of the system is monitored as Fig. 2B. Mean temperature is 100 K.

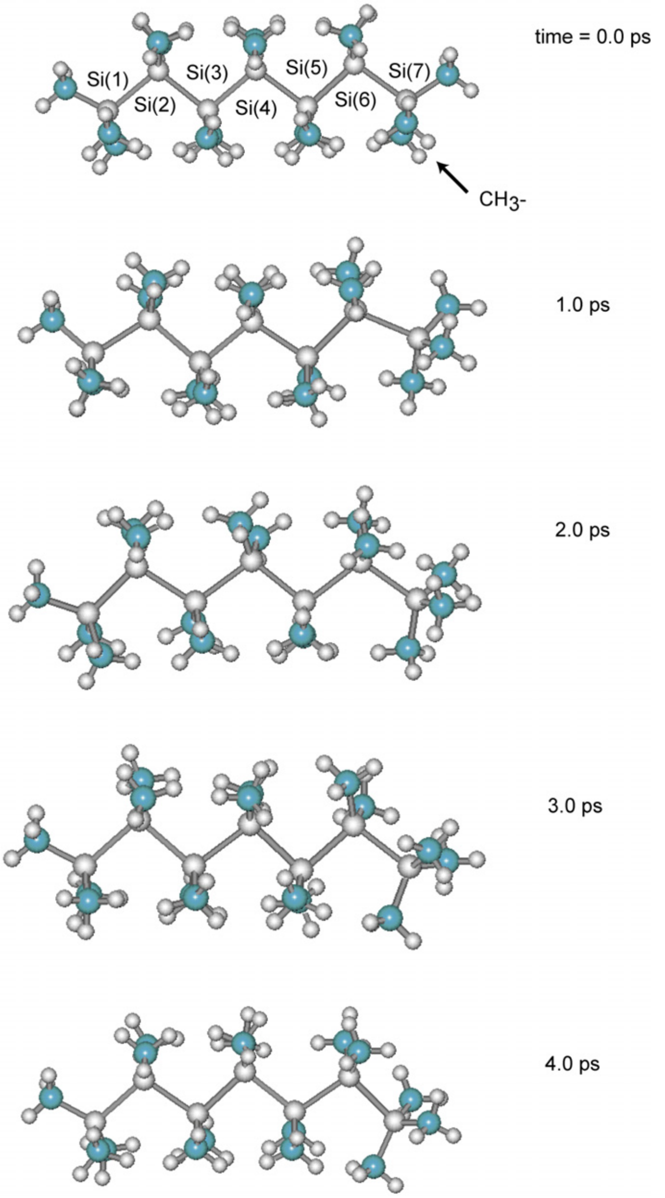

Fig. 1. Snapshots of structures of $Si_n(CH_3)_{2n+2}$ ($n = 7$) calculated using direct MO–MD method (PM3 level). Simulation temperature is 100 K.

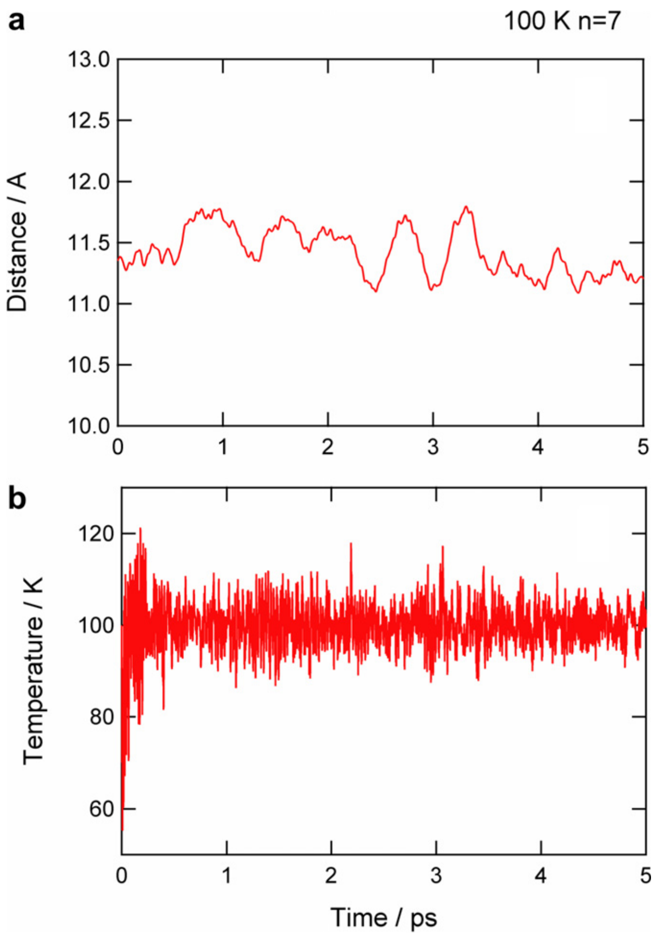

Fig. 2. Time-propagation of (a) head-to-tail distance, Si(1)–Si(7), and (b) temperature of the system obtained by direct MO–MD method.

Table 1
Optimized geometrical parameters of permethyloligosilane radical cations ($n = 4$–7) calculated at the B3LYP/3-21G(d) level

n	Dihedral angle/degree			
	Si(1–2–3–4)	Si(2–3–4–5)	Si(3–4–5–6)	Si(4–5–6–7)
4	163.1			
5	162.7	162.7		
6	160.3	171.7	169.4	
7	159.4	171.1	171.1	159.4

Table 2
Excitation energies of $Si_n(CH_3)_{2n+2}^+$ (in eV) calculated at the CIS/3-21G(d), TD-DFT(B3LYP)/3-21G(d), and TD-DFT(B3LYP)/6-311+G(d,p) levels of theory

State	4	5	6	7
CIS/3-21G(d)[a]				
1st	2.119 (0.2151)	2.048 (0.3259)	1.867 (0.4241)	1.719 (0.4981)
2nd	3.064 (0.0016)	3.179 (0.0000)	3.062 (0.0003)	3.050 (0.0005)
3rd	5.038 (0.0036)	3.310 (0.0113)	3.542 (0.0003)	3.283 (0.0166)
TD-DFT/3-21G(d)[a]				
1st	1.888 (0.1619)	1.762 (0.2791)	1.596 (0.4039)	1.439 (0.5159)
2nd	2.164 (0.0009)	2.169 (0.0001)	2.094 (0.0003)	1.980 (0.0008)
3rd	2.883 (0.0040)	2.287 (0.0202)	2.272 (0.0179)	2.196 (0.0090)
4th	2.901 (0.0022)	2.894 (0.0066)	2.344 (0.0003)	2.360 (0.0006)
5th	2.982 (0.0497)	2.907 (0.0002)	2.865 (0.0039)	2.380 (0.0021)
6th	3.061 (0.000)	3.003 (0.0282)	2.876 (0.0000)	2.840 (0.0011)
TD-DFT/6-311+G(d,p)[a]				
1st	1.849 (0.1584)			
2nd	2.132 (0.0009)			
3rd	2.833 (0.0040)			
4th	2.848 (0.0024)			
5th	2.922 (0.0508)			
6th	3.003 (0.0000)			
Expl.[b]	1.80	1.70	1.61	–

Oscillator strengths are given in parentheses.

[a] Structures are obtained by B3LYP/3-21G(d) calculation.

[b] First excitation energies (experimental values) are cited from Ref. [18].

The direct MO–MD calculations are carried out for $n = 4$–6. The similar feature is obtained.

Next, a number of seven structures in the time-range 1.0–2.5 ps are randomly selected from the result of the direct MO–MD calculation, and then the geometries are fully optimized at the B3LYP/3-21G(d) level. However, all calculations give the same total energy for the final structure and all structures have a regular all-*trans* form. This result strongly suggests that the structure of $Si_7(CH_3)_{16}$ vibrates abound the regular all-*trans* form and the effect of rotation of methyl groups is negligible small. The most stable structure is further optimized at the B3LYP/3-21G(d) level. The selected optimized structures are listed in Table 1. The dihedral angles are calculated to be in the range 160–170°. These results indicate that the optimizations for $n = 4$–7 give also all-transoid structures.

3.2. Electronic states of radical cations of oligosilanes ($n = 4$–7)

The first excitation energies of radical cations of oligosilanes calculated at the CIS/3-21G(d) and TD-DFT(B3LYP)/3-21G(d) level are given in Table 2 together with experimental data. The first excitation energy decreases with increasing chain length (n): the values for $n = 4$, 5, 6, and 7 are calculated to be 2.12, 2.05, 1.87, and 1.72 eV (CIS), respectively. The B3LYP calculations for $n = 4$, 5, 6, and 7 give 1.89, 1.76, 1.61, and 1.44 eV (B3LYP), respectively. Oscillator strengths are gradually increased. The corresponding experimental excitation energies for $n = 4$, 5, and 6 are 1.80. 1.70, and 1.60 eV, respectively. Thus, theoretical calculations at the CIS/3-21G(d) and B3LYP/3-21G(d) levels represent reasonably the experimental excitation energies.

To check the basis set dependency on the excitation energies and electronic states, the B3LYP/6-311+G(d,p) calculation is carried out for $n = 4$. The first excitation energy is calculated to be 1.85 eV, which is in good agreement with the values of the other levels. This result indicates that CIS/3-21G(d) and B3LYP/3-21G(d) calculations would give a reasonable electronic states of radical cation of oligosilane.

SAC-CI calculation is preliminary performed for radical cation of $n = 2$ to check the level of theory on the oscillator strength. The intensities (f) and excitation energies for the first and second electronic transitions are $f = 0.0$ (1.87 eV) and 0.021 (2.25 eV), respectively at the SAC-CI/3-21G(d) level. The corresponding values are $f = 0.0$ (1.53 eV) and 0.020 (1.90 eV). Thus, CIS calculation gives a reasonable oscillator strength of radical cation of oligosilane.

In the present study, we consider only $n = 4$–7 for radical cations of oligosilane. The first excitation energies for $n = 7$ is calculated to be 1.439 eV, which is low enough occur the hole transfer at thermal condition. To elucidate the effect of chain length on the band gap, the excitation energies are preliminary calculated for the oligosilanes with long chain. The band gaps for $n = 8$, 10, 16, 20, 26 are calculated to 1.28, 1.06, 0.65, 0.50, and 0.396 eV, respectively. These energies are sufficiently low for hole conductively at thermal condition.

3.3. Spin densities in oligosilane radical cation at the ground and low-lying excited states

To elucidate hole distribution at the ground and low-lying excited states, SE-CI calculations are carried out for $n = 4$–7. We consider two parts of oligosilane as regions of spin density distributions: these are spin densities in a part of Si–Si skeleton (Si main chain) and that of methyl groups (side chain). Spin densities condensed to two parts are plotted as a function of electronic state ($\boldsymbol{m}$) in Fig. 3, where notation of $\boldsymbol{m}$ means electronic state of oligosilane. For example, $\boldsymbol{m} = 0$ means the ground state, and $\boldsymbol{m} = 1$, 2, and 3 means the first, second, and third excited states, respectively.

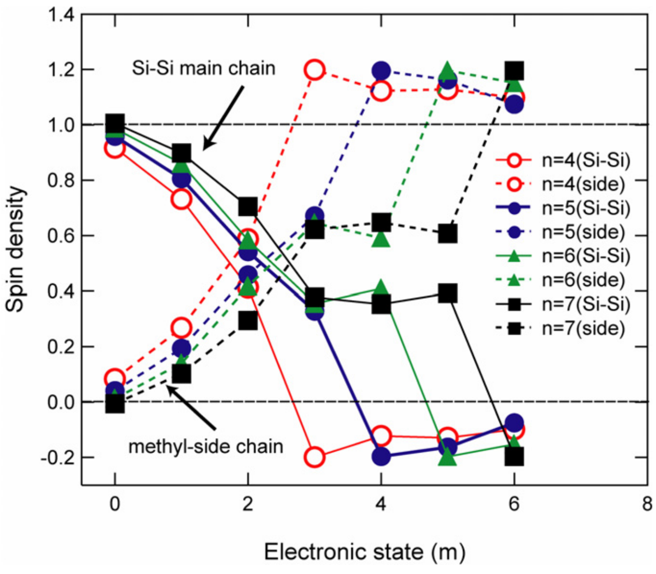

Fig. 3. Effects of electronic states on spin densities in main and side chains of oligosilane radical cation ($n = 4$–7) calculated at the CIS/3-21G(d) level. Notation $\boldsymbol{m}$ means electronic state of oligosilane radical cation, where $\boldsymbol{m} = 0$ means the ground state, and $\boldsymbol{m} = 1$, 2, and 3 are first, second and third excited states, respectively.

At the ground state of oligosilane radical cation ($\boldsymbol{m} = 0$, $n = 4$), spin densities on the Si–Si skeleton and methyl group are calculated to be 0.917 and 0.083, respectively, indicating that almost all hole is localized in the Si–Si skeleton, and spin densities on the methyl group is close to zero. In the case of longer chain length (for example, $\boldsymbol{m} = 0$, $n = 7$), the spin density on the main- and side-chains are 1.010 and −0.010, respectively, at the ground state. This indicates that spin separation at the ground state becomes larger at longer chain lengths.

At the first excited state ($\boldsymbol{m} = 1$, $n = 4$), the spin densities for the Si–Si main and side chains are 0.732 and 0.268, respectively, indicating that almost of hole is still remained in the Si–Si main chain, and about 25 % of hole is transferred to the side chain. At the second excited state ($\boldsymbol{m} = 2$, $n = 4$), spin densities for main- and side-chains are 0.413 and 0.587, respectively, suggesting that a large amount of hole is transferred from the Si–Si main chain to the methyl side chain at the second excited state. In the third excited state ($\boldsymbol{m} = 3$, $n = 4$), almost all hole is localized in the side chain, the spin densities are −0.199 in main chain and 1.199 in side chain.

In the case of radical cation with longer chain length ($n = 7$), spin densities on main and side chains are calculated to be 1.006 and −0.006 ($\boldsymbol{m} = 0$), 0.898 and 0.102 ($\boldsymbol{m} = 1$), 0.705 and 0.295 ($\boldsymbol{m} = 2$), and 0.378 and 0.622 ($\boldsymbol{m} = 3$). Thus, the distribution of the spin densities is drastically changed by the electronic state. These result strongly indicate that photo-excitation causes an intramolecular hole transfer within the radical cation of oligosilanes. Also, it is found that magnitude of hole transfer becomes stronger in longer chain lengths of oligosilanes.

To visualize these electronic state, spin densities at both ground and excited states are illustrated by iso-surface in Fig. 4. At the ground state, the unpaired electron is delocalized along the Si–Si skeleton and there is no spin density on the CH_3 side chain. The distribution of the spin density corresponds approximately to shape of singly occupied molecular orbital (SOMO). At the first excited state, the spin orbital is also close of that of ground state because the first excited state is composed of single electron excited state expressed by a transition from SOMO-1 to SOMO. At the second excited state, half of unpaired electron is transferred from the main chain to the side chain. The spin density distribution is fully localized in the side chain at higher excited states. Thus, it is found that spin distribution is drastically changed by the electronic states.

Here we consider the effect of substitution of side group on the distribution of spin density. The spin densities of radical cation of methylphenyloligosilane (2 unit model) are calculated with same manner. The unpaired electron is widely distributed in both main- and side-chains (phenyl group) even at the ground state. This is due to the fact that hole is delocalized between Si–Si main chain and phenyl group by σ–π interaction. This feature is in good agreement with previous experiments [16,23].

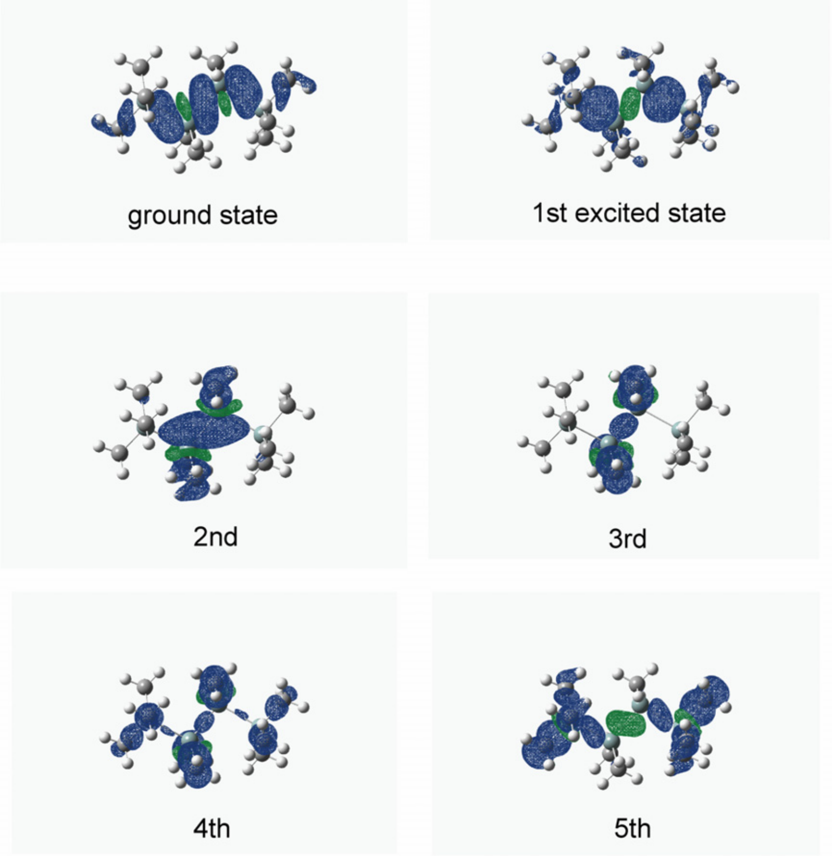

Fig. 4. Illustration of spin densities of oligosilane radical cation at the ground state and low-lying excited states.

As mentioned in introduction, the effects of the substitution of the side group on the efficiency of hole transfer were measured by Seki et al. They found that the substitution of side group from alkyl to phenyl groups increases drastically the efficiency of hole transfer at the ground state. From our calculations and their experiment, it is concluded that the methyl group in radical cation of oligosilane plays a role to insulate the electron hopping between polymer chains.

4. Discussion

4.1. Summary

In the present study, ab initio CI and TD-DFT calculations were applied to the permethyloligosilane radical cations $Si_n(CH_3)_{2n+2}^+$ ($n = 4$–7) to elucidate the electronic states at both ground and excited states. The spin densities (hole) at the ground and first excited states are delocalized along the Si–Si main chain. On the other hand, the hole is transferred from the Si–Si main chain to the side-chain at the second and higher excited states.

The model of hole transfer in oligosilane radical cation with alkyl groups is schematically illustrated in Fig. 5. At the ground and first excited states, hole is delocalized along the Si–Si main chain. This result strongly indicates that hole is transferred along the Si–Si backbone at thermal condition. Polysilane radical cation with alkyl groups in side chain will play as one-dimensional quantum wire. The present calculation predicted that hole is transferred to the side chain at the second and higher excited states if lifetime of the excited state is long enough to the second photo-irradiation. From these results, it can be predicted that the intermolecular hole transfer takes place by photo-irradiation to the radical cation. Namely, it is suggested that the polysilane radical cation plays as two-dimensional quantum wire at the excited states by photo-excitation. Thus, the present calculation predicts the new mechanism for the hole transfer under the photo-irradiation.

4.2. Estimation of hole conductivity between polymer chains

Here, we estimate roughly the ratio of hole conductivities at the ground and electronic excited states. The magnitude of hole conductivity between polymer chains is dominant mainly by both the reorganization energy of oligosilane (λ) and coupling of orbital energies between chains (Δ) [24]. The hole conductivity (J) is proportional to a ratio of the reorganization energy (λ) and the coupling (Δ), $J \approx \Delta^2 \lambda^{-1/2}$, which is an important factor to estimate the hole hopping between polymer chains. Here, it is assumed that this relation is valid in both ground and excited states. The reorganization energy (λ) is estimated by the stabilization energy of $Si_n(Me)_{2n+2}^+$ ($n = 6$) after the hole capture

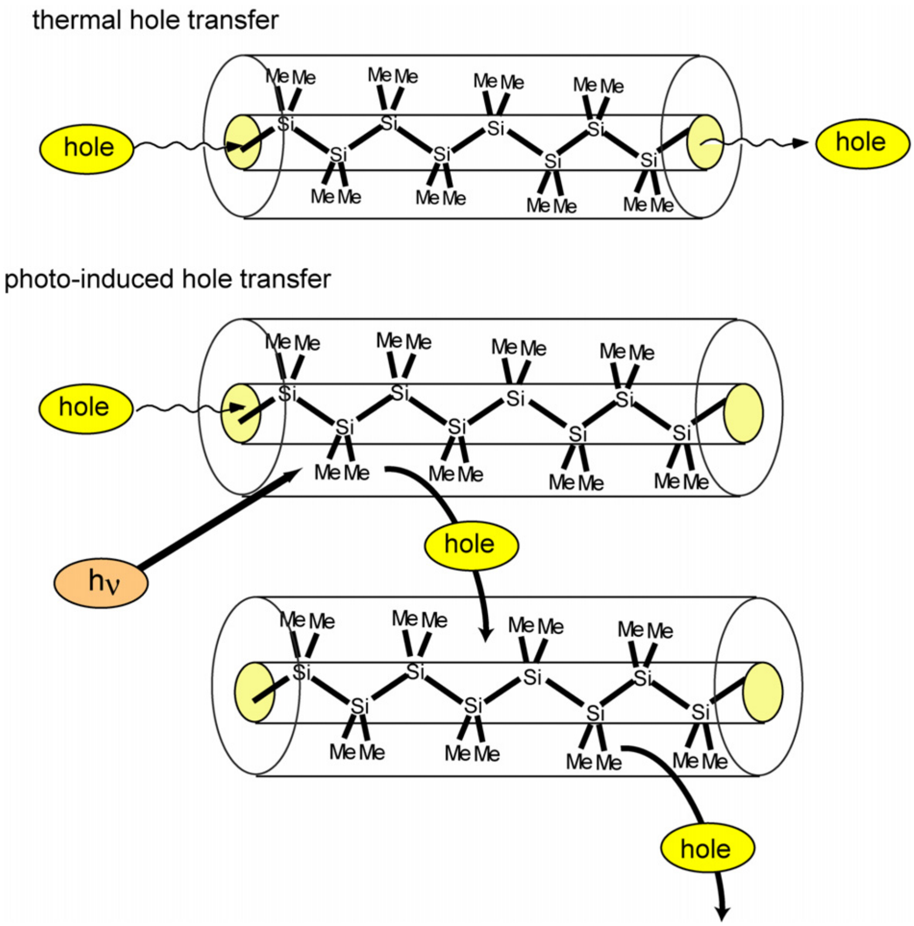

Fig. 5. Models of hole transport in oligosilane radical cation: (top) hole transport ay thermal condition, and (bottom) hole transport caused by photo-irradiation.

of its neutral state. Vertical ionization energy of $n = 6$ is calculated to be 7.18 eV and adiabatic ionization potential is 6.78 eV at the B3LYP/6-311+G(d,p) level, indicating that the reorganization energy is 0.40 eV. The magnitude of orbital coupling (Δ) is estimated by a shift of orbital energy. In this calculation, a system composed of two neutral oligosilane ($n = 6$) is used as a model. Interchain distance between Si atoms is assumed to 6.5 Å, which is a normal packing distance. It should be noted that the coupling is varied at its electronic states (ground, first and second excited sates). The coupling calculations are carried out at the PM3 level with two chains of $Si_n(Me)_{2n+2}$. The magnitudes of couplings are calculated to be 3.0×10^{-2} eV ($=\Delta$) for the ground state and 0.47 eV ($=\Delta^*$) for the excited state. Hence, ratio of hole conductivities at ground and excited states (J^*) is roughly estimated to be $J^*/J \approx (\Delta^*)^2/\Delta^2 = 250$. This value suggest that the hole conductivity is lager at the excited state than that of ground state. The ratio is of course obtained qualitatively using the simple relation, while one need more accurate calculation using the explicit equation to gain a realistic value for the ratio. However, at least, it can be concluded that the hole conductivity more increases at the excited state than that of ground state. This is originated from that the spin density (hole density) increases in the side-chain at the excited states and the interaction becomes stronger.

Acknowledgements

The authors are indebted to the Computer Center at the Institute for Molecular Science (IMS) for the use of the computing facilities. Also, the authors acknowledges a partial support from President's optional budget from Kyoto University. One of the authors (H.T.) acknowledges a partial support from a Grant-in-Aid for Scientific Research (C) from the Japan Society for the Promotion of Science (JSPS).

References

[1] R. Miller, D. Michl, J. Chem. Rev. 89 (1989) 1359.
[2] T. Ogawa, A. Yamaguchi, T. Soga, H. Tachibana, M. Matsumoto, H. Oizumi, E. Takeda, Jpn. J. Appl. Phys. 33 (1994) 1577.
[3] F.K. Perkins, E.A. Dobisz, S.L. Brandow, J.M. Calvert, J.E. Kosakowski, C.R.K. Marrian, Appl. Phys. Lett. 68 (1996) 550.
[4] R. Hattori, T. Sugano, J. Shirafuji, T. Fujiki, Jpn. J. Appl. Phys. 35 (1996) L1509.

[5] H. Suzuki, S. Hoshino, C.H. Yuan, M. Fujiki, S. Toyoda, N. Matsumoto, IEEE J. Quantum Electron. 4 (1998) 129.
[6] H. Suzuki, S. Hoshino, C.H. Yuan, M. Fujiki, S. Toyoda, N. Matsumoto, Thin Solid Films 331 (1998) 64.
[7] Y. Xu, T. Fujino, S. Watase, H. Naito, K. Oka, T. Dohmaru, Jpn. J. Appl. Phys. 38 (1999) 2609.
[8] H. Suzuki, S. Hoshino, K. Furukawa, K. Ebata, C.H. Yuan, I. Bleyl, Polym. Adv. Technol. 11 (2000) 460.
[9] K. Okamoto, T. Tojo, H. Tada, M. Terazima, K. Matsushige, Mol. Cryst. Liquid Cryst. 370 (2001) 379.
[10] M. Hiramoto, Y. Sakata, M. Yokoyama, Jpn. J. Appl. Phys. 35 (1996) 4809.
[11] R.G. Kepler, J.M. Zeigler, L.A. Harrah, S.R. Kurtz, Phys. Rev. B 35 (1987) 2818.
[12] M.A. Abkowitz, M.J. Rice, M. Stolka, Philos. Mag. 61 (1990) 25.
[13] G.P. Van de Laan, M.P. De Haas, J.M. Marman, H. Frey, M. Möller, Mol. Cryst. Liquid Cryst. 236 (1993) 65.
[14] H. Frey, M. Möller, M.P. De Haas, N.J.P. Zenden, P.G. Schouten, G.P. Van de Laan, M.P. De Haas, J.M. Marman, Macromolecules 26 (1993) 89.
[15] G.P. Van de Laan, M.P. De Haas, A. Hummel, H. Frey, S. Scheiko, M. Möller, Macromolecules 27 (1994) 1897.
[16] S. Seki, Y. Koizumi, T. Kawaguchi, H. Habara, S. Tagawa, J. Am. Chem. Soc. 126 (1989) 3521.
[17] S. Irie, M. Irie, Macromolecules 25 (1992) 1766.
[18] J. Kumagai, H. Tachikawa, H. Yoshida, T. Ichikawa, J. Phys. Chem. 100 (1996) 16777.
[19] H. Tachikawa, A. Shimizu, J. Phys. Chem. B 109 (2005) 13255.
[20] M.J. Frisch, G.W. Trucks, H.B. Schlegel, G.E. Scuseria, M.A. Robb, J.R. Cheeseman, J.A. Montgomery Jr., T. Vreven, K.N. Kudin, J.C. Burant, J.M. Millam, S.S. Iyengar, J. Tomasi, V. Barone, B. Mennucci, M. Cossi, G. Scalmani, N. Rega, G.A. Petersson, H. Nakatsuji, M. Hada, M. Ehara, K. Toyota, R. Fukuda, J. Hasegawa, M. Ishida, T. Nakajima, Y. Honda, O. Kitao, H. Nakai, M. Klene, X. Li, J.E. Knox, H.P. Hratchian, J.B. Cross, C. Adamo, J. Jaramillo, R. Gomperts, R.E. Stratmann, O. Yazyev, A.J. Austin, R. Cammi, C. Pomelli, J.W. Ochterski, P.Y. Ayala, K. Morokuma, G.A. Voth, P. Salvador, J.J. Dannenberg, V.G. Zakrzewski, S. Dapprich, A.D. Daniels, M.C. Strain, O. Farkas, D.K. Malick, A.D. Rabuck, K. Raghavachari, J.B. Foresman, J.V. Ortiz, Q. Cui, A.G. Baboul, S. Clifford, J. Cioslowski, B.B. Stefanov, G. Liu, A. Liashenko, P. Piskorz, I. Komaromi, R.L. Martin, D.J. Fox, T. Keith, M.A. Al-Laham, C.Y. Peng, A. Nanayakkara, M. Challacombe, P.M.W. Gill, B. Johnson, W. Chen, M.W. Wong, C. Gonzalez, J.A. Pople, Gaussian 03, Revision B.04, Gaussian, Inc., Pittsburgh, PA, 2003.
[21] H. Tachikawa, H. Kawabata, J. Mater. Chem. 13 (2003) 1293.
[22] H. Tachikawa, H. Kawabata, J. Phys. Chem. B 107 (2003) 1113.
[23] H. Tachikawa, H. Kawabata, J. Phys. Chem. B 109 (2005) 3139.
[24] E. Johsnasson, S. Larsson, Synth. Metal. 144 (2004) 183.